Research Article Vol. 27, No. 15 / 22 July 2019 / Optics Express 21810

Optics EXPRESS

High-accuracy and wide dynamic range frequency-based dispersion spectroscopy in an optical cavity

AGATA CYGAN,[*] PIOTR WCISŁO, SZYMON WÓJTEWICZ, GRZEGORZ KOWZAN, MIKOŁAJ ZABOROWSKI, DOMINIK CHARCZUN, KATARZYNA BIELSKA, RYSZARD S. TRAWIŃSKI, ROMAN CIURYŁO, PIOTR MASŁOWSKI, AND DANIEL LISAK

Institute of Physics, Faculty of Physics, Astronomy and Informatics, Nicolaus Copernicus University in Toruń, Grudziadzka 5, Torun 87-100, Poland
[*] *agata@fizyka.umk.pl*

Abstract: A spectroscopic method free from systematic errors is desired for many challenging applications of gas detection. Although existing cavity-enhanced techniques exhibit very high precision, their accuracy strongly depends on propagation of the light amplitude through an optical system and its detection. Here, we demonstrate that the frequency-based molecular dispersion spectroscopy, involving sub-Hz-level precision in frequency measurements of optical cavity resonances, leads to sub-per-mille accuracy and a wide dynamic range, both previously unattainable by any other spectroscopic technique. The method offers great sensitivity of $5{\times}10^{-11}$ cm^{-1}, high speed, limited only by the fundamental response time of the cavity, and traceability of both axes of the spectrum to the primary frequency standard. All these features are necessary for convenient realization of comprehensive molecular spectroscopy from Doppler up to collisional regime without changing the spectroscopic method and modification of the experimental setup. Moreover, the presented approach does not require linear, high-bandwidth nor phase-sensitive detectors and can be directly implemented in existing cavity-enhanced spectrometers utilizing either continuous-wave or coherent broadband radiation. We experimentally prove the predominance of frequency-based spectroscopy over intensity-based one. Our results motivate replacement of intensity-based absorption spectroscopy with a pure frequency-based dispersion one in applications where the highest accuracy is required.

1. Introduction

The extremely high precision of ultrasensitive spectroscopic techniques highlights the critical role played by the accuracy of measurement methods in many important scientific areas. A serious challenge for remote sensing, important in global warming monitoring and for understanding climate change, among others, is to measure variations in gas composition with accuracy better than 0.1% [1,2]. Modelling of exoplanetary atmospheres [3,4] and searching for extraterrestrial life [5] both need a consistent description of the millions of lines resulting from hot atmospheres of exoplanets. These scientific tasks require reference data which can only be provided by calculations supported and verified by critical high-accuracy measurements [4]. High-quality laboratory spectra are necessary for better theoretical description of molecular structure [6,7], isotope ratio determination [8,9], fundamental tests of QED in molecular systems [10] and searching for new physics beyond the Standard Model [11]. Because of its great sensitivity and precision, cavity ring-down spectroscopy (CRDS) is widely used for all these applications. However, various effects related to light propagation and detection, e.g., insufficient extinction ratios of optical switches [12], a multimode [13] or slightly non-resonant [14] excitations of cavity modes, nonlinear and limited-bandwidth detection system [15] affect the accuracy of

#360603
Journal © 2019
https://doi.org/10.1364/OE.27.021810
Received 21 Feb 2019; revised 21 Jun 2019; accepted 27 Jun 2019; published 19 Jul 2019

CRDS and restrict its applicability to weakly absorbing systems. A way to extend the dynamic range of measurements is to probe cavity mode widths instead of ring-down decays. Although cavity mode-width spectroscopy (CMWS) [16,17] does not require high-bandwidth detectors as CRDS, its accuracy can still be diminished by detector nonlinearity, cavity length jitter [16,18] and finite spectral linewidth of the laser [19].

The recently introduced cavity mode-dispersion spectroscopy (CMDS) [20] has an intrinsic advantage over other techniques. It relies on pure frequency measurements of cavity mode positions and thus avoids accuracy limitations typical of most methods with intensity-dependent detection. An alternative technique, NICE-OHMS [21], provides dispersive spectra of the highest precision. However, its sensitivity to calibration of the enhancement factor and the need for careful phase adjustment during demodulation of the resulting signal lead to systematic errors of line-shape parameters even up to several percent [22]. A different variant of NICE-OHMS, dual-frequency modulation dispersion spectroscopy [23], enables continuous monitoring of dispersive changes of the cavity free spectral range (FSR). Although this technique is frequency-based as CMDS, its accuracy is limited by measurement of the averaged values of the FSR.

In the previous state-of-the-art CMDS experiment [20], a laser beam was polarization-divided into lock and probe beams. A robust laser-to-cavity lock provided great spectral resolution with a Hz-level linewidth laser and eliminated the residual frequency noise associated with mutual vibrations of the laser and cavity. Active stabilization of the cavity length prevented the comb of cavity modes from thermally drifting. In order to measure the cavity mode shape, the probe beam was frequency stepped with respect to the locking point by tuning an optical frequency shifter (i.e. acoustooptic modulator). With this approach a sub-Hz-level precision of both cavity mode positions and widths [20] was achieved. This gives the CMDS method a high place among ultrasensitive spectroscopic techniques. Furthermore, the method's frequency-based detection could plausibly reach metrological level of accuracy, indicating its strong potential to be the most robust technique with respect to systematic errors. The technical issues limiting the accuracy of CMDS and leading to distorted dispersive spectra [24] resulted from the requirement of efficient spectral separation of locking and probe beams, and a potential contribution from residual amplitude modulation. The latter typically occurs in the Pound-Drever-Hall locking scheme during frequency changes of the laser [25] and was responsible for a slow drift of the laser-to-cavity locking point [26]. We present a CMDS method using a high-bandwidth electrooptic modulator (EOM) as a fast tunable coherent light source (Fig. 1), which eliminates these limitations and allows CMDS to approach the level of sub-per-mille accuracy. Our solution improves the stability of the laser-to-cavity lock by keeping the frequency of the lock beam constant during the entire spectrum measurement, and provided a convenient relative frequency axis of the spectrum in the low microwave range, which is easily referenced to a primary frequency standard. Moreover, setting the locking point far enough from the measured molecular resonance prevented the laser-to-cavity lock from being affected by absorption [24] and significantly expanded the dynamic range of measurements. In the presented method each spectrum scan is a series of cavity pumping processes grouped around consecutive cavity mode centers. The processes are equidistant in time and the frequencies at which they occur are determined by the frequency of the lock beam and the offset introduced by the microwave frequency driving the EOM. Similarly to rapid absorption spectroscopy methods [27,28], fast frequency switching of the microwave source reduced data acquisition time to the fundamental cavity pumping rate. However, unlike a frequency-agile, rapid scanning spectroscopy technique [27], our method provides exact positions of cavity mode centers leading to complete and accurate information on the molecular spectrum.

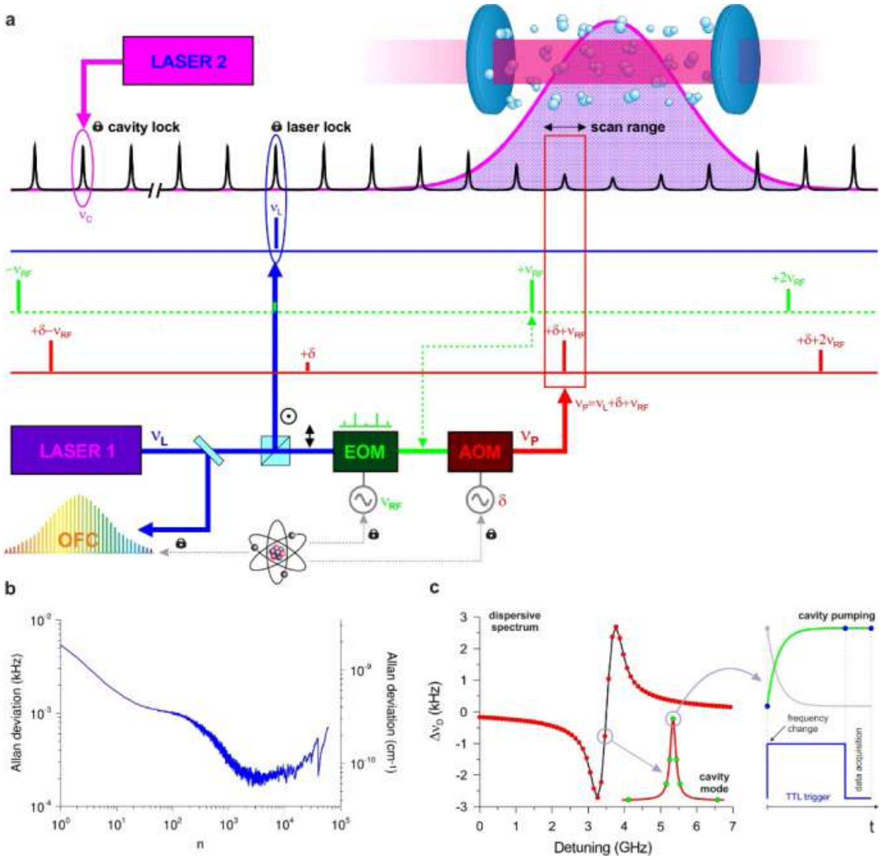

Fig. 1. Diagram of universal experimental setup for implementation of methods: CRDS, CMWS and CMDS. (a) A beam of laser 1 with frequency ν_L is divided into three parts. The first one is sent to the optical frequency comb (OFC) in order to monitor the frequency stability of the laser and to provide an absolute frequency axis for measurements. The second one, vertically polarized, is used to tightly phase-lock the laser to the optical cavity resonance. The third one, horizontally polarized, is first modulated by the high-bandwidth electrooptical modulator (EOM) with the radiofrequency ν_{RF} and next frequency shifted by the acoustooptic modulator driven by the radiofrequency δ. The single sideband of the EOM is used as a probe beam for measuring cavity mode shapes in case of CMWS and CMDS methods. The AOM is used both to prevent pumping the cavity with carrier frequency and other EOM sidebands, as well as to initiate ring-down decays in the CRDS. The experimental conditions are chosen so that at any given moment, only one cavity mode was excited. The OFC, EOM and AOM are frequency referenced to a primary atomic standard. The comb of cavity modes is actively stabilized to the frequency ν_C of laser 2. (b) Allan deviation of measured mode positions of empty cavity in frequency and absorption units (n – number of measurements). Time interval between measurements was 3 ms. The plot minimum corresponds to detection limit of 5×10^{-11} cm^{-1}. (c) High-speed measurement procedure of dispersive spectrum. Each spectrum scan is a series of equidistant in time processes of cavity pumping corresponding to various EOM radiofrequencies ν_{RF} grouped around consecutive cavity mode centers. A gray decay shows the process of cavity emptying from the light for previous radiofrequency ν_{RF} which starts just after the EOM frequency change.

2. Experimental details

The experimental realization of CRDS, CMWS and CMDS methods is provided by the two-beam configuration system presented in Fig. 1. The gas sample is placed inside the temperature-stabilized [29] optical cavity with finesse 41000 and free spectral range (FSR) 203 MHz corresponding to mirror reflectivity 0.999923 and cavity length 74 cm. The sample is illuminated by 1560 nm light from an external-cavity diode laser (ECDL). Active stabilization of the comb of cavity modes with respect to the I_2-stabilized Nd:YAG laser (Laser 2, *Innolight Prometheus*) working at 1.06 µm prevents thermal drift of the cavity length. Long term stability of the Nd:YAG laser measured with respect to the optical frequency comb (OFC, *Menlo Systems*) is 4×10^{-14} at 100 s [30]. The ECDL (Laser 1, *Toptica CTL 1550*) is remotely tunable in the range 1.52–1.63 µm and Pound-Drever-Hall locked to one of the cavity modes. Its spectral line width relative to the cavity mode center is on the order of tens of Hz [30]. A separated beam of the ECDL is phase-modulated by the electrooptic modulator (EOM, *Photline Technologies*) in a wide frequency range from 200 MHz to 20 GHz. A selected first-order (+1 or −1) sideband of the EOM serves as a probe light. The AOM used in the system prevents pumping the cavity with the carrier and other EOM sidebands. It also initiates ring-down decays in the CRDS. EOM sidebands can be tuned with a maximal speed of 1.4 kHz corresponding to an RF switching time of 700 us. The high-speed scan of the EOM is enabled to cover the spectral range up to ± 20 GHz. Spectroscopy in a wider spectral range can be realized by automatic and remotely controlled relocking of the ECDL to another cavity mode. Cavity mode widths and positions are typically measured with Hz-level precision, but presence of 1/f noise allows square root data averaging towards sub-Hz-level precision. Under signal-to-noise ratios as high as 2000, cavity mode shapes are well reproduced by the Lorentzian function. For every point of CMWS and CMDS spectrum, 5 cavity mode shapes were measured with a step-size ranging from 375 Hz up to 1.25 kHz depending on the sample pressure. Alternatively, without signal averaging a fast spectra acquisition can be realized, as shown in Fig. 1(c). In this case one frequency step of the spectrum takes 3 ms (7 points per each cavity mode) and is limited only by the cavity response time. Ring-down decays in CRDS were initiated exactly from the cavity mode centers by quickly (within 50 ns) switching off the laser beam using an acoustooptic modulator. For every spectral point of CRDS spectrum 3 000 decays were acquired. Controlled tuning of the Nd:YAG laser frequency, to which the cavity is locked, enables measurement of the absorption and dispersion spectra, also with a step-size smaller than the cavity FSR, limited by the Nd:YAG laser stability. The total measurement time during which all three CRDS, CMWS and CMDS spectra were acquired was 16 minutes for the lowest pressure and 27 minutes for the highest pressure to preserve the spectrum length proportional to the line width.

The absolute frequency axis in the experiment is calculated by summing the lock beam frequency ν_L, offset frequency δ of the AOM and offset frequency ν_{RF} of the microwave source driving the EOM. The frequency ν_L is continuously measured with respect to the OFC. Its absolute value is determined on the basis of the carrier envelope offset frequency, comb repetition rate frequency (f_{rep} = 250 MHz) and beatnote frequency with the nearest OFC tooth in a similar way as in papers [30,31]. Integer number of the comb tooth is determined by measuring the lock beam frequency ν_L by a wavelength meter (*Bristol*) whose accuracy is better than $f_{\mathrm{rep}}/2$. The UTC (Coordinated Universal Time) reference used to stabilize the OFC, AOM and EOM is provided by the Astro-Geodynamic Observatory in Borowiec (Poland) and transfered to the experiment by the OPTIME fiber network [30,32]. Its overall relative stability is 10^{-15} after 8 h [32]. The offset frequency $\delta + \nu_{\mathrm{RF}}$ corresponds to the frequency difference measured between lock beam and center of the cavity mode shifted by dispersion. The accuracy of this measurement is affected by the cavity length stability. Based on results from [30] we estimate that maximal contribution of this effect to the combined uncertainty of $\delta + \nu_{\mathrm{RF}}$ is 38 mHz in 10 s, which is the time required for 5 cavity mode measurements per each spectrum point.

3. Data analysis

Measured spectral line shapes were analysed at atmospheric conditions where line shape model requires simultaneous inclusion [33,34] of Dicke narrowing [35] and speed-dependence of collisional broadening and shifting [36]. The Levenberg-Marquardt algorithm was implemented for the least squares fitting. Line-shape models were numerically calculated with a relative accuracy of 10^{-6}. When the Voigt profile was employed for spectral analysis, the fitted parameters were: unperturbed line position, collisional line width, collisional line shift, integrated line area, and background parameters. In the case of the HTP, four additional parameters were used: Dicke narrowing, speed dependence of collisional width and shift, and first order line mixing. For both profiles, Doppler widths were fixed to the values calculated on the basis of the measured temperature. The spectrum background was modeled by the linear function. At obtained signal-to-noise ratio we did not observe any systematic distortions of the background caused by etalon effects. We also estimated potential contribution of the mirror dispersion to the spectrum background based on the results of broadband comb-based spectroscopy from Refs. [18] and [37]. Linear contribution is fully fitted in our background model, whereas nonlinear contribution in case of the longest measured spectrum (16 GHz) should be below 50 mHz and 140 mHz based on data from [37] and [18], respectively. This is below the noise level of our spectra. Due to longer line wings in the dispersive spectrum compared to absorptive one, analysis of CMDS spectra required incorporation of 9 neighboring lines up to 200 GHz away from the investigated one. To quantify an agreement between the fitted line-shape model and experimental data, we used a quality of the fit factor (QF) defined as a ratio of the peak absorption/dispersion to the standard deviation of the fit residuals [38].

The wave number and line intensity for the investigated self-perturbed R23 CO transition provided by the HITRAN database [34] are $\widetilde{\nu}_0 = 6410.87956 \ \text{cm}^{-1}$ and $S = 7.843 \times 10^{-25}$ cm/molec, respectively. The measured CO line was analysed by means of the single and multi-spectrum fit. In the first approach, the spectra were fitted individually for every pressure and separate line-shape parameter sets were provided. In the second approach, all pressure-dependent spectra were fitted together, providing one parameter set including pressure-dependent linear coefficients of line-shape parameters [40,41]. This approach enables us to solve a common problem of numerical correlations between parameters that are present when sophisticated multi-parameter line-shape models such as HTP are used. Due to the precision of spectra measurements being greater than the accuracy of the pressure gauge employed to make pressure measurements, in the multi-spectrum fit the collisional widths and line areas were fitted separately for every pressure. For other parameters such as unperturbed line position, collisional shifting coefficient, Dicke narrowing coefficient, line-mixing coefficient and speed-dependent parameters describing collisional width and shift, single values were fitted for all pressures. For the case of determination of unperturbed line position and collisional shift three methods of data analysis were used and each method was applied to two sets of data. The first set included only low pressures, up to 0.5 kPa, and the second one included all investigated pressures, up to 54 kPa. The first and most straightforward method involved performing single-spectrum fits of all lines in the set and applying linear regression to line positions determined for each pressure. In this analysis it was necessary to include the speed-dependent collisional shift. However, a parameter describing the quadratic speed dependence is strongly correlated with the averaged collisional shift. Therefore two steps of analysis were done. After first one the collisional shift was obtained from the linear regression and it was next used as a fixed parameter in final single-spectrum fit analysis, from which the unperturbed line position was determined. The two remaining methods incorporated the multi-spectrum fit analysis in which single values of the unperturbed line position and collisional shift coefficient were fitted simultaneously for all pressures, but they differed in their approach to the collisional shift coefficient. In the first one of these multi-spectrum fit methods the collisional shift was fitted, whereas in the second one it was fixed to the best value obtained from the multi-spectrum fit analysis of CMDS spectra in the full range of pressures. The latter method helps to efficiently reduce correlations between line position and collisional shift which are present at low pressure range even when the multi-spectrum fit procedure is applied (see Fig. 4). If experimental spectra are free from systematic distortions we should get the same value of the unperturbed line position and collisional shift from all methods, except for potential numerical correlations between these parameters at very low pressure range.

4. Results

In order to demonstrate the extraordinary accuracy and extremely wide dynamic range of the CMDS method, we compared it with two absorptive methods: CRDS, which is well established in ultra-sensitive measurements, and CMWS, its equivalent in the frequency domain. The dispersive and absorptive spectra corresponding to these techniques, shown in Fig. 2, were obtained simultaneously by the use of the experimental setup from Fig. 1. The chosen R23 CO transition is strong enough to test the accuracy of experimental methods at pressures ranging from Doppler up to collisional regime, corresponding to conditions from low to high optical density. The measurement conditions were chosen to be far from light power saturation. The data fitting was performed with the Hartmann-Tran profile (HTP), a new recommended standard for interpretation of Earth's atmosphere retrievals [42], which is capable of reproducing spectra with accuracy better than 0.1% in a wide pressure range up to atmospheric conditions [43].

The accuracy of the CRDS method noticeably decreases for high absorptions, where ring-down decays become non-exponential [12] and too short for their proper measurement. In our experimental conditions this situation already occurs for CO pressure of 2 kPa, corresponding to ring-down time constant of 1.5 μs, and is revealed as a large (∼1.6% peak to peak) structure on the residuals from the HTP fit (Fig. 2). This precludes the use of CRDS for accurate wide dynamic range line shape study, which is crucial for, e.g. atmospheric applications. In case of CMWS increase of absorption causes decrease of the signal amplitude, similar as in CRDS, but contrary to it, broadened cavity modes in CMWS can still be measured with satisfactory accuracy. Indeed, a single-spectrum fit analysis applied to the CMWS spectra resulted in structureless (<0.2% peak to peak) residuals in the whole investigated range of pressures (Fig. 2). It is worth noting that even at high optical density conditions, at pressures of 13 kPa and 54 kPa, corresponding to reduction of the cavity transmission by more than 10^4, CMWS spectra have very high signal-to-noise ratio of around 6 000. Comparison of the results for CRDS and CMWS methods at pressure 2 kPa reveals that CRDS underestimates the line intensity by more than 3%. On the other hand, for pressures above 2 kPa the line intensities obtained in CMWS systematically deviate from the constant value by between 0.2% and 0.8% (Fig. 3) and the results for line positions are scattered within ±130 kHz dependent on the kind of data analysis and chosen pressure range (Fig. 4). These observations indicate a possible systematic error of the CMWS method even if the residuals from the fit appear to be randomly distributed. In case of the single-spectrum fit analysis with a flexible multi-parameter line-shape model such as the HTP, any distortions of the spectrum can be misinterpreted as a physically justified collisional effect. The multi-spectrum fit analysis forces a linear dependence of parameters on pressure and helps to solve this problem. Its application to the CMWS spectra indeed showed a presence of a small asymmetric structure on residuals for the lowest pressures. We ascribe this asymmetry to a variable frequency noise in the locking of the laser to the cavity, which influences the measured mode widths but not the mode centers.

As shown in Fig. 2, the multi-spectrum analysis applied to the CMDS spectra provides the highest quality residuals from the HTP fit. The achieved quality of the fit factor QF = 17 000 is more than double that of CMWS. The ultra-high accuracy of the CMDS method is proven by (i) randomly distributed, non-asymmetric residuals in the whole investigated range of pressures (Fig. 2), (ii) pressure independence of the line intensity within the desired accuracy range

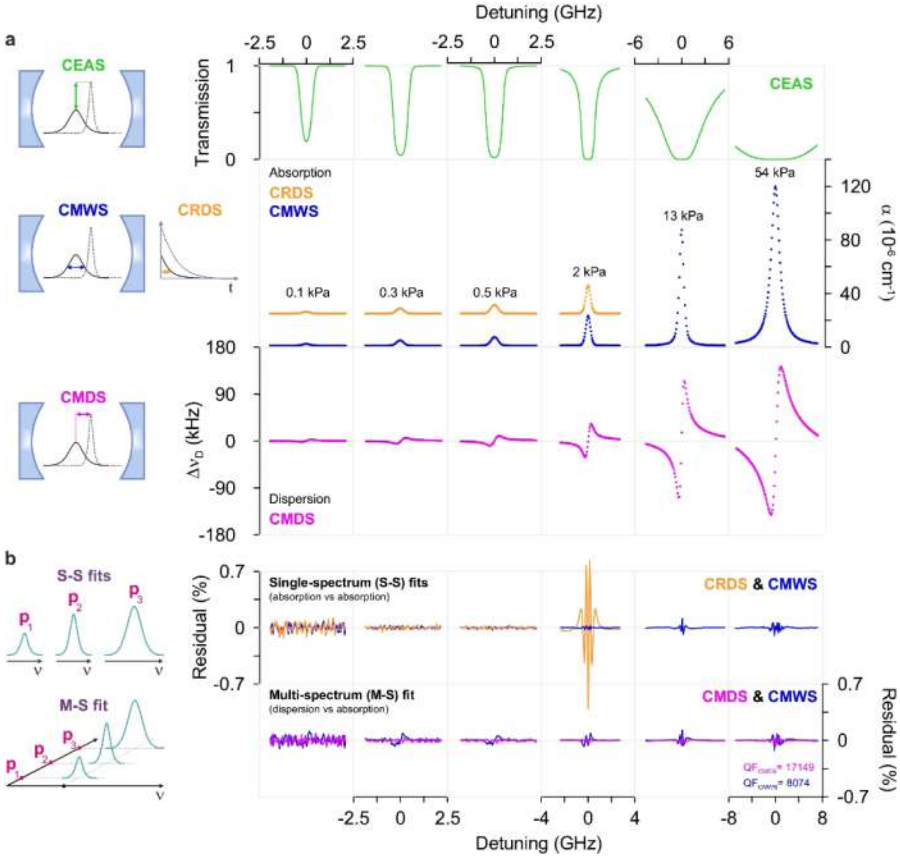

Fig. 2. Absorption and dispersion cavity-enhanced spectroscopy. The shown R23 transition in the second overtone of CO was measured at the room temperature and indicated pressures by three cavity-enhanced spectroscopy methods: CRDS, CMWS and CMDS. (a) Top: simulation of cavity transmission in direct cavity-enhanced absorption spectroscopy (CEAS). Middle: absorption spectra measured by CRDS and CMWS. For clarity, the CRDS data were moved up slightly. Bottom: dispersion spectra measured by CMDS. Every spectrum in the pressure range 0.1-2 kPa is the average of 10 scans. Spectra for pressures 13 kPa and 54 kPa are the average of 20 scans. (b) Upper: comparison of CRDS and CMWS residuals obtained from the single-spectrum fit analysis. Lower: comparison of CMDS and CMWS residuals obtained from the multi-spectrum fit analysis. Standard deviation of CMDS low-pressure residuals corresponds to absorption of 5×10^{-10} cm^{-1}. The Hartmann-Tran profile with collisional line mixing was used to model spectra for all investigated methods. In the single-spectrum analysis, spectra were fitted individually for every pressure, whereas in the multi-spectrum analysis all spectra were fitted together with forced linear pressure dependence of chosen line-shape parameters. CRDS results are limited to low pressures. Above the pressure of 2 kPa, ring-downs are too short for accurate measurement, which leads to the large structure in residuals from the fit. CMWS and CMDS spectra expose the wide dynamic range of absorption and dispersion measurements, respectively. The small instrumental asymmetry affecting CMWS spectra, well masked in the case of the single-spectrum analysis, can be detected by the multi-spectrum fit technique. Among the three studied methods, CMDS represents the highest standard in providing ultra-accurate laboratory spectra. For quantitative comparison of CMWS and CMDS results, the quality of the fit factors (QF) from the multi-spectrum fit analysis are given. Horizontal axes and pressures are common for each column of plots (a) and (b).

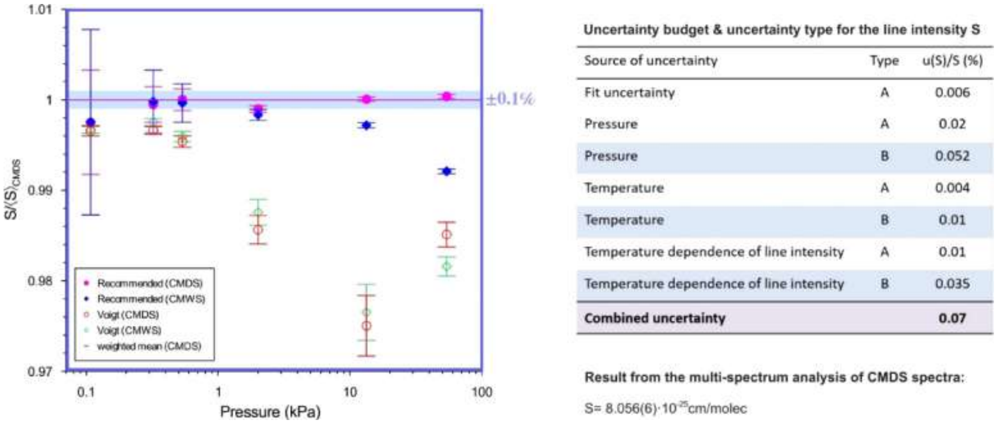

Uncertainty budget & uncertainty type for the line intensity S

Source of uncertainty	Type	u(S)/S (%)
Fit uncertainty	A	0.006
Pressure	A	0.02
Pressure	B	0.052
Temperature	A	0.004
Temperature	B	0.01
Temperature dependence of line intensity	A	0.01
Temperature dependence of line intensity	B	0.035
Combined uncertainty		**0.07**

Result from the multi-spectrum analysis of CMDS spectra:

$S= 8.056(6)\cdot 10^{-25}$cm/molec

Fig. 3. Line intensity of R23 CO transition. Line intensities obtained from CMWS and CMDS spectra are shown. Full circles and diamonds: Intensities provided by the multi-spectrum analysis with use of the recommended Hartmann-Tran profile with collisional line mixing. The results for CMWS and CMDS agree up to 0.04% for low pressures and systematically disagree by 0.2% to 0.8% above pressures of 2 kPa, due to instrumental errors affecting the CMWS method. CMDS shows an excellent constancy of the line intensity with pressure. Open circles and diamonds: Intensities provided by the single spectrum analysis with the use of the ordinary Voigt profile. The results present strong nonphysical dependence on pressure and inaccuracies of up to 3% caused by use of a too-simplified line-shape model. Plotted intensities are normalized to the mean value with the lowest uncertainty obtained in CMDS. Error bars on graph correspond to combined standard uncertainties. The uncertainty budget of the line intensity, including type A (statistical) and type B (other) components, achieved from the multi-spectrum analysis of CMDS spectra is shown.

of ± 0.1% (Fig. 3), and (iii) independence of the line position determination of the method of data analysis and the choice of pressure range (Fig. 4). Although the reported here line intensity was determined with a very low combined standard uncertainty of 0.07%, its value $\mathbf{8.056 \times 10^{-25} cm/molec}$ differs by as much as + 2.6% from the line intensity provided with uncertainty <2% by the HITRAN database [39] and by + 1.9% from the line intensity measured with uncertainty 1.6% by Sung and Varanasi [44]. These examples demonstrate a problem of inaccuracies of spectroscopic databases as well as indicate an urgent need for development of high-accuracy spectroscopic methods and proper analysis of laboratory spectra.

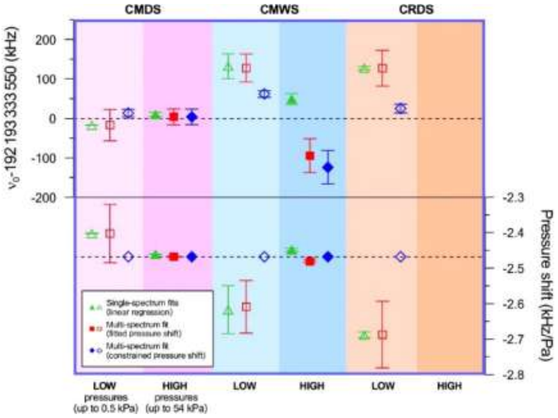

Uncertainty budget & uncertainty type for the line position (ν_0) and collisional shift (δ)

Source of uncertainty	Type	$u(\nu_0)$ (kHz)	$u(\delta)/\delta$ (%)
Fit uncertainty	A	20	0.06
Pressure	B	< 0.81	0.052
Combined uncertainty		**20**	**0.08**

Results from the multi-spectrum analysis of CMDS spectra:

ν_0= 192193333554(20) kHz
δ = -2.468(2) kHz/Pa

Fig. 4. Line position and collisional shift of R23 CO transition. Unperturbed line positions and shifts obtained from CMDS, CMWS and CRDS spectra are shown for various methods of data analysis employed to two ranges of pressures. In the case of the single spectrum analysis (triangles), the results were determined from the linear regression. In the first multi-spectrum analysis (squares), one value of the line position and pressure shift coefficient was fitted for all pressures. In the second multi-spectrum analysis (diamonds), the pressure shift coefficient was constrained to the best value determined from the first high-pressure range multi-spectrum analysis of CMDS spectra. Experimental spectra were fitted by the Hartman-Tran profile. The results for CMDS agree within their standard fit uncertainties with each other for all pressures. The results for CMWS are scattered due to the systematic errors of this method. CRDS results are limited to low pressures and agree with CMWS low-pressure results. Correlations between line positions and line shifts occur at low pressures for all investigated methods, but CMDS shows the greatest resistance to it. Error bars on graph correspond to combined standard uncertainties. The uncertainty budget of the line position and collisional shift, including type A (statistical) and type B (other) components, achieved from the multi-spectrum analysis of CMDS spectra is shown.

5. Conclusions

We have shown that a unique feature of CMDS is its accuracy - the parameter of the highest priority in modern laboratory modelling of Doppler-limited molecular spectra affected by collisions. Detection of the dispersive signal in terms of microwave frequencies also meets the highest metrology standards. The demonstrated wide dynamic range of CMDS, unattainable by any other ultra-sensitive spectroscopy technique, spans from 5×10^{-10} cm^{-1} up to 10^{-4} cm^{-1} (Fig. 2). It enables the most stringent tests of the molecular collision theory. Using the example of a self-broadened CO line, we have shown that CMDS can provide line intensities with relative uncertainties well below 0.1% in the wide range of absorptions, up to atmospheric pressures. On the other hand, the high sensitivity of CMDS enables detection of absorption as low as 5×10^{-11} cm^{-1} (Fig. 1(b)). Obtained precision of 6×10^{-5} of the line intensity, which is an order of magnitude better than dominant systematic contribution to combined uncertainty coming from a pressure gauge, opens a way for high-precision spectroscopic measurements of pressure. We also proved that it is possible to obtain unperturbed line positions with the relative uncertainty of 10^{-10} from Doppler-broadened spectra in conditions where molecular collisions are far from negligible. The R23 CO line position determined here ($\boldsymbol{\nu_0}$ **= 192 193 333 554(20)** kHz) agrees very well with and is 15 times more accurate than the results published elsewhere [45]. Moreover, the line position uncertainty of our CO transition is comparable with the most precise sub-Doppler measurements of HD transitions of similar line strength [46,47]. It would be very interesting to use CMDS to explain large systematic differences between the results for HD line positions obtained in various laboratories using cavity-enhanced absorption techniques [46,47]. Additionally this is to our knowledge the first time when the self-induced collisional shift ($\boldsymbol{\delta} = \mathbf{-2.468(2)}$ kHz/Pa) of investigated line was determined with sub-per mille accuracy. The CMDS method does not require linear, high-bandwidth nor phase-sensitive detectors, provides both axes of the spectrum referenced to the primary frequency standard and can be directly implemented in existing cavity-enhanced spectrometers utilizing either continuous-wave or coherent broadband radiation [18,48,49]. We see clear applications of CMDS in atmospheric and astrophysics research as a reference method for a new generation of spectroscopic databases, in molecular chemistry as well as in accurate metrology of molecular hydrogen and fundamental studies. The presented results can be in general approach a part of a paradigm shift to frequency-based dispersion spectroscopy from intensity-based absorption one thanks to its immunity to systematic errors.

Note added before publication: Recently we were informed that the similar relative accuracy of the line intensity has been reached using CRDS with properly calibrated detection system [50].

Funding

Narodowe Centrum Nauki (NCN) (2014/15/D/ST2/05281, 2015/17/B/ST2/02115, 2015/18/E/ST2/00585, 2015/19/D/ST2/02195, 2016/21/N/ST2/00334, 2016/23/B/ST2/00730, 2017/24/T/ST2/00242, DEC-2013/11/D/ST2/02663); European Cooperation in Science and Technology (COST) (CM1405 MOLIM).

Acknowledgments

The authors would like to thank Dr. Mateusz Borkowski for language corrections of the manuscript. The research is part of the program of the National Laboratory FAMO in Torn, Poland, supported by the subsidy of the Ministry of Science and Higher Education.

References

1. K. R. Gurney, R. M. Law, A. S. Denning, P. J. Rayner, D. Baker, P. Bousquet, L. Bruhwiler, Y.-H. Chen, P. Ciais, S. Fan, I. Y. Fung, M. Gloor, M. Heimann, K. Higuchi, J. John, T. Maki, S. Maksyutov, K. Masarie, P. Peylin, M. Prather, B. C. Pak, J. Randerson, J. Sarmiento, S. Taguchi, T. Takahashi, and C.-W. Yuen, "Towards robust regional estimates of CO_2 sources and sinks using atmospheric transport models," Nature **415**(6872), 626–630 (2002).
2. D. R. Thompson, D. C. Benner, L. R. Brown, D. Crisp, V. Malathy Devi, Y. Jiang, V. Natraj, F. Oyafuso, K. Sung, D. Wunch, R. Castaño, and C. E. Miller, "Atmospheric validation of high accuracy CO_2 absorption coefficients for the OCO-2 mission," J. Quant. Spectrosc. Radiat. Transfer **113**(17), 2265–2276 (2012).
3. A. S. Burrows, "Highlights in the study of exoplanet atmospheres," Nature **513**(7518), 345–352 (2014).
4. P. F. Bernath, "Molecular opacities for exoplanets," Phil. Trans. R. Soc. A **372**(2014), 20130087 (2014).
5. S. Seager and W. Bains, "The search for signs of life on exoplanets at the interface of chemistry and planetary science," Sci. Adv. **1**(2), e1500047 (2015).
6. S. Yu, C. E. Miller, B. J. Drouin, and H. S. Müller, "High resolution spectral analysis of oxygen. I. Isotopically invariant Dunham fit for the $X^3\Sigma_g{}^-$, $a^1\Delta_g$, $b^1\Sigma_g{}^+$ states," J. Chem. Phys. **137**(2), 024304 (2012).
7. O. L. Polyansky, K. Bielska, M. Ghysels, L. Lodi, N. F. Zobov, J. T. Hodges, and J. Tennyson, "High-accuracy CO_2 line intensities determined from theory and experiment," Phys. Rev. Lett. **114**(24), 243001 (2015).
8. I. Galli, S. Bartalini, S. Borri, P. Cancio, D. Mazzotti, P. De Natale, and G. Giusfredi, "Molecular gas sensing below parts per trillion: radiocarbon-dioxide optical detection," Phys. Rev. Lett. **107**(27), 270802 (2011).
9. S. Koulikov, S. Assonov, A. Fajgelj, and P. Tans, "Potential improvements aimed at high precision $\delta^{13}C$ isotopic ratio determinations in CO_2 mixtures using optical absorption spectrometry," Talanta **184**, 73–86 (2018).
10. E. J. Salumbides, G. D. Dickenson, T. I. Ivanov, and W. Ubachs, "QED Effects in Molecules: Test on Rotational Quantum States of H_2," Phys. Rev. Lett. **107**(4), 043005 (2011).
11. E. J. Salumbides, J. C. J. Koelemeij, J. Komasa, K. Pachucki, K. S. E. Eikema, and W. Ubachs, "Bounds on fifth forces from precision measurements on molecules," Phys. Rev. D **87**(11), 112008 (2013).
12. H. Huang and K. K. Lehmann, "Noise caused by a finite extinction ratio of the light modulator in CW cavity ring-down spectroscopy," Appl. Phys. B: Lasers Opt. **94**(2), 355–366 (2009).
13. J. T. Hodges, J. P. Looney, and R. D. van Zee, "Response of a ring-down cavity to an arbitrary excitation," J. Chem. Phys. **105**(23), 10278–10288 (1996).
14. S. Wójtewicz, A. Cygan, J. Domysławska, K. Bielska, P. Morzyński, P. Masłowski, R. Ciuryło, and D. Lisak, "Response of an optical cavity to phase-controlled incomplete power switching of nearly resonant incident light," Opt. Express **26**(5), 5644 (2018).

15. S. Wójtewicz, D. Lisak, A. Cygan, J. Domysławska, R. Trawiński, and R. Ciuryło, “Line-shape study of self-broadened O_2 transitions measured by Pound-Drever-Hall-locked frequency-stabilized cavity ring-down spectroscopy,” Phys. Rev. A **84**(3), 032511 (2011).
16. A. Cygan, D. Lisak, P. Morzyński, M. Bober, M. Zawada, E. Pazderski, and R. Ciuryło, “Cavity mode-width spectroscopy with widely tunable ultra-narrow laser,” Opt. Express **21**(24), 29744 (2013).
17. D. A. Long, G.-W. Truong, R. D. van Zee, D. F. Plusquellic, and J. T. Hodges, “Frequency-agile, rapid scanning spectroscopy: absorption sensitivity of 2×10^{-12} $\mathrm{cm}^{-1}\mathrm{Hz}^{-1/2}$ with a tunable diode laser,” Appl. Phys. B: Lasers Opt. **114**(4), 489–495 (2014).
18. L. Rutkowski, A. C. Johansson, G. Zhao, T. Hausmaninger, A. Khodabakhsh, O. Axner, and A. Foltynowicz, “Sensitive and broadband measurement of dispersion in a cavity using a Fourier transform spectrometer with kHz resolution,” Opt. Express **25**(18), 21711 (2017).
19. K. Nakagawa, T. Katsuda, A. S. Shelkovnikov, M. de Labachelerie, and M. Ohtsu, “Highly sensitive detection of molecular absorption using a high finesse optical cavity,” Opt. Commun. **107**(5-6), 369–372 (1994).
20. A. Cygan, P. Wcisło, S. Wójtewicz, P. Masłowski, J. T. Hodges, R. Ciuryło, and D. Lisak, “One-dimensional frequency-based spectroscopy,” Opt. Express **23**(11), 14472 (2015).
21. J. Ye, L.-S. Ma, and J. L. Hall, “Ultrasensitive detections in atomic and molecular physics: demonstration in molecular overtone spectroscopy,” J. Opt. Soc. Am. B **15**(1), 6 (1998).
22. J. Wang, P. Ehlers, I. Silander, and O. Axner, “On the accuracy of the assessment of molecular concentration and spectroscopic parameters by frequency modulation spectrometry and NICE-OHMS,” J. Quant. Spectrosc. Radiat. Transfer **136**, 28–44 (2014).
23. F. M. Schmidt, W. Ma, A. Foltynowicz, and O. Axner, “Highly sensitive dispersion spectroscopy by probing the free spectral range of an optical cavity using dual-frequency modulation,” Appl. Phys. B: Lasers Opt. **101**(3), 497–509 (2010).
24. A. Cygan, S. Wójtewicz, M. Zaborowski, P. Wcisło, R. Guo, R. Ciuryło, and D. Lisak, “One-dimensional cavity mode-dispersion spectroscopy for validation of CRDS technique,” Meas. Sci. Technol. **27**(4), 045501 (2016).
25. N. C. Wong and J. L. Hall, “Servo control of amplitude modulation in frequency-modulation spectroscopy: demonstration of shot-noise-limited detection,” J. Opt. Soc. Am. B **2**(9), 1527 (1985).
26. A. Cygan, D. Lisak, S. Wójtewicz, J. Domysławska, R. S. Trawiński, and R. Ciuryło, “Active control of the Pound-Drever-Hall error signal offset in high-repetition-rate cavity ring-down spectroscopy,” Meas. Sci. Technol. **22**(11), 115303 (2011).
27. G.-W. Truong, K. O. Douglass, S. E. Maxwell, R. D. van Zee, D. F. Plusquellic, J. T. Hodges, and D. A. Long, “Frequency-agile, rapid scanning spectroscopy,” Nat. Photonics **7**(7), 532–534 (2013).
28. J. Burkart, D. Romanini, and S. Kassi, “Optical feedback stabilized laser tuned by single-sideband modulation,” Opt. Lett. **38**(12), 2062 (2013).
29. M. Zaborowski, P. Wcisło, F. Thibault, S. Wójtewicz, A. Cygan, G. Kowzan, P. Masłowski, D. Lisak, and R. Ciuryło, “Ultra accurate measurements and ab initio calculations of collisional effects in pure D_2,” J. Phys.: Conf. Ser. **810**, 012042 (2017).
30. A. Cygan, S. Wójtewicz, G. Kowzan, M. Zaborowski, P. Wcisło, J. Nawrocki, P. Krehlik, Ł. Śliwczyński, M. Lipiński, P. Masłowski, R. Ciuryło, and D. Lisak, “Absolute molecular transitions frequencies measured by three cavity-enhanced spectroscopy techniques,” J. Chem. Phys. **144**(21), 214202 (2016).
31. S. Wójtewicz, A. Cygan, P. Masłowski, J. Domysławska, D. Lisak, R. S. Trawiński, and R. Ciuryło, “Spectral line shapes of self-broadened P-branch transitions of oxygen B band,” J. Quant. Spectrosc. Radiat. Transfer **144**, 36–48 (2014).
32. P. Morzyński, M. Bober, D. Bartoszek-Bober, J. Nawrocki, P. Krehlik, Ł. Śliwczyński, M. Lipiński, P. Masłowski, A. Cygan, P. Dunst, M. Garus, D. Lisak, J. Zachorowski, W. Gawlik, C. Radzewicz, R. Ciuryło, and M. Zawada, “Absolute measurement of the $^1S_0 - {}^3P_0$ clock transition in neutral ^{88}Sr over the 330 km-long stabilized fibre optic link,” Sci. Rep. **5**(1), 17495 (2015).
33. R. Ciuryło and J. Szudy, “Speed-dependent pressure broadening and shift in the soft collision approximation,” J. Quant. Spectrosc. Radiat. Transfer **57**(3), 411–423 (1997).
34. A. S. Pine, “Asymmetries and correlations in speed-dependent Dicke-narrowed line shapes of argon-broadened HF,” J. Quant. Spectrosc. Radiat. Transfer **62**(4), 397–423 (1999).
35. R. H. Dicke, “The effect of collisions upon the Doppler width of spectral lines,” Phys. Rev. **89**(2), 472–473 (1953).
36. P. R. Berman, “Speed-dependent collisional width and shift parameters in spectral profiles,” J. Quant. Spectrosc. Radiat. Transfer **12**(9), 1331–1342 (1972).
37. D. Charczun, G. Kowzan, A. Cygan, R. S. Trawiński, D. Lisak, and P. Masłowski, “Broadband and high resolution measurements of cavity loss and dispersion,” Photonics Lett. Pol. **10**(2), 48 (2018).
38. A. Cygan, D. Lisak, S. Wójtewicz, J. Domysławska, J. T. Hodges, R. S. Trawiński, and R. Ciuryło, “High signal-to-noise ratio laser technique for accurate measurements of spectral line parameters,” Phys. Rev. A **85**(2), 022508 (2012).
39. I. E. Gordon, L. S. Rothman, C. Hill, R. V. Kochanov, Y. Tan, P. F. Bernath, M. Birk, V. Boudon, A. Campargue, K. V. Chance, B. J. Drouin, J.-M. Flaud, R. R. Gamache, J. T. Hodges, D. Jacquemart, V. I. Perevalov, A. Perrin, K. P. Shine, M.-A. H. Smith, J. Tennyson, G. C. Toon, H. Tran, V. G. Tyuterev, A. Barbe, A. G. Császár, V. M. Devi, T. Furtenbacher, J. J. Harrison, J.-M. Hartmann, A. Jolly, T. J. Johnson, T. Karman, I. Kleiner, A. A. Kyuberis, J.

Loos, O. M. Lyulin, S. T. Massie, S. N. Mikhailenko, N. Moazzen-Ahmadi, H. S. P. Müller, O. V. Naumenko, A. V. Nikitin, O. L. Polyansky, M. Rey, M. Rotger, S. W. Sharpe, K. Sung, E. Starikova, S. A. Tashkun, J. Vander Auwera, G. Wagner, J. Wilzewski, P. Wcisło, S. Yu, and E. J. Zak, "The HITRAN2016 molecular spectroscopic database," J. Quant. Spectrosc. Radiat. Transfer **203**, 3–69 (2017).

40. D. C. Benner, C. P. Rinsland, V. M. Devi, M. A. H. Smith, and D. Atkins, "A multispectrum nonlinear least squares fitting technique," J. Quant. Spectrosc. Radiat. Transfer **53**(6), 705–721 (1995).
41. A. S. Pine and R. Ciuryło, "Multispectrum fits of Ar-broadened HF with a generalized asymmetric lineshape: effects of correlation, hardness, speed dependence, and collision duration," J. Mol. Spectrosc. **208**(2), 180–187 (2001).
42. J. Tennyson, P. F. Bernath, A. Campargue, A. G. Csaszar, L. Daumont, R. R. Gamache, J. T. Hodges, D. Lisak, O. V. Naumenko, L. S. Rothman, H. Tran, N. F. Zobov, J. Buldyreva, C. D. Boone, M. D. De Vizia, L. Gianfrani, J.-M. Hartmann, R. McPheat, D. Weidmann, J. Murray, N. H. Ngo, and O. L. Polyanski, "Recommended isolated-line profile for representing high-resolution spectroscopic transitions (IUPAC Technical Report)," Pure Appl. Chem. **86**(12), 1931–1943 (2014).
43. D. Lisak, A. Cygan, D. Bermejo, J. L. Domenech, J. T. Hodges, and H. Tran, "Application of the Hartmann-Tran profile to analysis of H_2O spectra," J. Quant. Spectrosc. Radiat. Transfer **164**, 221–230 (2015).
44. K. Sung and P. Varanasi, "Intensities, collision-broadened half-widths, and collision-induced line shifts in the second overtone band of $^{12}C^{16}O$," J. Quant. Spectrosc. Radiat. Transfer **83**(3-4), 445–458 (2004).
45. D. Mondelain, T. Sala, S. Kassi, D. Romanini, M. Marangoni, and A. Campargue, "Broadband and highly sensitive comb-assisted cavity ring down spectroscopy of CO near 1.57 µm with sub-MHz frequency accuracy," J. Quant. Spectrosc. Radiat. Transfer **154**, 35–43 (2015).
46. L.-G. Tao, A.-W. Liu, K. Pachucki, J. Komasa, Y. R. Sun, J. Wang, and S.-M. Hu, "Toward a determination of the proton-electron mass ratio from the Lamb-dip measurement of HD," Phys. Rev. Lett. **120**(15), 153001 (2018).
47. F. M. J. Cozijn, P. Dupre, E. J. Salumbides, K. S. E. Eikema, and W. Ubachs, "Sub-Doppler frequency metrology in HD for tests of fundamental physics," Phys. Rev. Lett. **120**(15), 153002 (2018).
48. A. C. Johansson, L. Rutkowski, A. Filipsson, T. Hausmaninger, G. Zhao, O. Axner, and A. Foltynowicz, "Broadband calibration-free cavity-enhanced complex refractive index spectroscopy using a frequency comb," Opt. Express **26**(16), 20633 (2018).
49. G. Kowzan, D. Charczun, A. Cygan, R. S. Trawiński, D. Lisak, and P. Masłowski, "Broadband optical cavity mode measurements at Hz-level precision with a comb-based VIPA spectrometer," Sci. Rep. **9**(1), 8206 (2019).
50. A. J. Fleisher, E. M. Adkins, Z. D. Reed, H. Yi, D. A. Long, H. M. Fleurbaey, and J. T. Hodges, "Twenty-five-fold reduction in measurement uncertainty for a molecular line intensity," *Phys. Rev. Lett.* (accepted for publication).